ISSN 1063-7850, Technical Physics Letters, 2018, Vol. 44, No. 6, pp. 541–544. © Pleiades Publishing, Ltd., 2018.
Original Russian Text © V.A. Gritsenko, Yu.N. Novikov, A. Chin, 2018, published in Pis'ma v Zhurnal Tekhnicheskoi Fiziki, 2018, Vol. 44, No. 12, pp. 81–88.

Short-Range Order and Charge Transport in SiO_x: Experiment and Numerical Simulation

V. A. Gritsenko[a, b, c]*, Yu. N. Novikov[a], and A. Chin[d]

[a] *Rzhanov Institute of Semiconductor Physics, Siberian Branch, Russian Academy of Sciences, Novosibirsk, 630090 Russia*
[b] *Novosibirsk State University, Novosibirsk, 630090 Russia*
[c] *Novosibirsk State Technical University, Novosibirsk, 630090 Russia*
[d] *National Chiao Tung University, Hsinchu, Taiwan, Republic of China*
**e-mail: grits@isp.nsc.ru*

Received March 1, 2018

Abstract—The structure of nonstoichiometric silicon oxide (SiO_x) has been studied by the methods of high-resolution X-ray photoelectron spectroscopy and fundamental optical-absorption spectroscopy. The conductivity of SiO_x ($x = 1.4$ and 1.6) films has been measured in a wide range of electric fields and temperatures. Experimental data are described in terms of the proposed SiO_x structure model based on the concept of fluctuating chemical composition leading to nanoscale fluctuations in the electric potential. The maximum amplitude of potential fluctuations amounts to 2.6 eV for electrons and 3.8 eV for holes. In the framework of this model, the observed conductivity of SiO_x is described by the Shklovskii–Efros theory of percolation in inhomogeneous media. The characteristic spatial scale of potential fluctuations in SiO_x films is about 3 nm. The electron-percolation energy in $SiO_{1.4}$ and $SiO_{1.6}$ films is estimated to be 0.5 and 0.8 eV, respectively.

DOI: 10.1134/S1063785018060196

Amorphous nonstoichiometric silicon oxide (a-SiO_x) is a key dielectric in modern microelectronics. By varying the chemical composition of SiO_x, it is possible to change its optical and electrical properties, including photoluminescence (PL) [1], within broad limits. The optical spectra of SiO_x films depend to a considerable degree on the presence of embedded silicon nanoclusters, and the optical properties of these films are determined by the concentration and size of Si-nanoclusters [2]. Passivating SiO_x layers are used in poly-Si contacts of solar cells [3], nonvolatile memory based on localized charge storage [4], and resistive memory devices [5].

The present work was aimed at an experimental investigation of the short-range order in SiO_x films by means of high-resolution X-ray photoelectron spectroscopy (HRXPS), measurement of their fundamental optical-absorption spectra, elucidation of the mechanism of charge transport, and estimation of the characteristic spatial size and amplitude of potential fluctuations in terms of the Shklovskii–Efros percolation theory.

Samples of about 100-nm-thick a-SiO_x layers were synthesized by the method of chemical-vapor deposition method based on the interaction of SiH_4 and N_2O vapors at 640°C. The SiO_x-layer composition could be changed by varying the SiH_4/N_2O flux ratio. The films were deposited onto [100]-oriented *n*-type silicon substrates with a resistivity of ~10 Ω cm. The HRXPS spectra of $SiO_{1.4}$ films were measured using a Kratos AXIS-HS system with a source of monochromated AlK_α radiation. The spectra of optical absorption in the visible and near-IR frequency range were recorded on Shimadzu UV-300 and Specord S-300 UV-Vis spectrophotometers. Current–voltage (*I*–*V*) characteristics were measured using SiO_x film samples with deposited aluminum contacts of 5×10^{-3} cm^2 area.

In the literature, the structures of nonstoichiometric compounds are usually described in terms of the random-bonding (RB) or random-mixture (RM) models [6]. The RB model assumes that SiO_x consists of $SiO_\nu Si_{4-\nu}$ tetrahedra of five kinds (ν = 0, 1, 2, 3, and 4) and probability W_ν^{RB} of finding a ν-th-type tetrahedron (i.e., the fraction of these tetrahedra) in SiO_x with composition x is defined as [6]

$$W_\nu^{RB}(x) = \frac{4!}{\nu!(4-\nu)!}\left(\frac{x}{2}\right)^\nu\left(1-\frac{x}{2}\right)^{4-\nu}. \qquad (1)$$

According to the RM model, SiO_x consists of two phases: amorphous silicon (a-Si) and SiO_2 (i.e., of $SiSi_4$ and SiO_4 tetrahedra, respectively), the fractions of which are determined as $W_0^{RM}(x) = 1 - x/2$ and $W_4^{RB}(x) = x/2$, respectively.

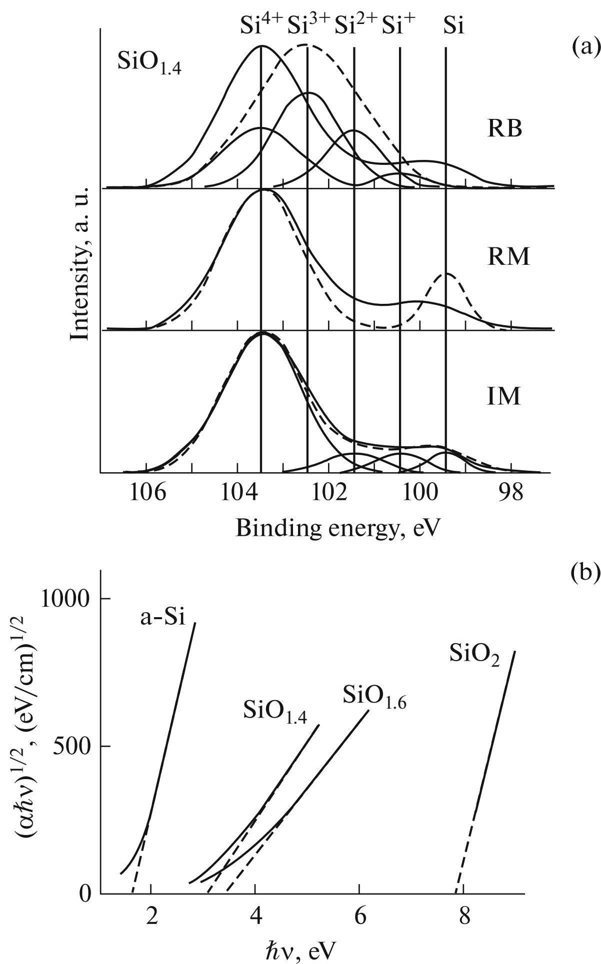

Fig. 1. (a) Experimental photoelectron spectra of Si 2p levels in $SiO_{1.4}$ (solid curves) and results of numerical simulation using RB, RM, and IM models (dashed curves); (b) spectral dependences of light absorption in SiO_x films with $x = 0$, 1.4, 1.6, and 2 (SiO_2 spectrum reproduced from [7]).

The photoelectron energy spectrum $I(E)$ is described using W_ν peaks defined in the RB and RM models broadened with Gaussian function by the following formula:

$$I(E) = \sum_{\nu} W_\nu e^{(E-E_\nu)^2/(2\sigma_\nu^2)}, \qquad (2)$$

where E_ν and σ_ν are the peak energy and half-width, respectively, for tetrahedra of the νth type.

Figure 1a shows the experimental photoelectron spectra of Si 2p levels in SiO_x (solid curves). The peak of Si^{4+} with binding energy E_0 = 103.5 eV and half-width σ_0 = 1.2 eV refers to the a-SiO_2 phase; the peak of Si with binding energy E_4 = 99.5 eV, and half-width σ_4 = 0.6 eV refers to the a-Si phase, while the binding energies and half-widths of the peaks for Si^{3+}, Si^{2+}, and Si^+ are determined by linear interpolation of E_0, E_4, σ_0, and σ_4 values with the corresponding numbers of oxygen atoms.

The top panel in Fig. 1a compares the experimental spectrum (solid curve) of Si 2p levels to the results of numerical simulation using the RB model (dashed curve). The latter Si 2p spectrum has a single peak with a binding energy of 102.5 eV. The maximum contribution to the calculated spectrum is due to SiO_x, while the contributions from SiO_2 and Si are underestimated. Calculation of the Si 2p spectrum using the RM model (Fig. 1a, middle panel) predicts the existence of two peaks corresponding to SiO_2 and Si phases. This calculation overestimates the contribution due to Si phase and underestimates the contribution of SiO_x phase. Thus, neither the RM nor RB model adequately describes the experimental photoelectron spectrum.

To describe the experimental HRXPS data, we propose to use an intermediate model (IM), according to which SiO_x consists of tetrahedra of five kinds (similarly to the RB model), but the distribution of these tetrahedral differs from that given by formula (1) for the RB model. In the proposed IM model, fractions W_ν of $SiO_\nu Si_{4-\nu}$ tetrahedra of five kinds (ν = 0, 1, 2, 3, and 4) are selected so as to ensure the best fit of the experimental spectrum to the $I(E)$ spectrum calculated by the Newton method using formula (2). Proper selection of the contributions of various types of tetrahedral provided good coincidence of the result of calculations to experiment (Fig. 1a, bottom panel).

For determining the bandgap width of SiO_x films, we have measured the spectra of fundamental optical absorption. Figure 1b presents spectral dependences of the optical absorption edge for a-Si, a-SiO_x, and SiO_2 films (the spectrum of SiO_2 was taken from [7]). The absorption edge of SiO_x varies within 3.1–3.4 eV.

Comparison of the simulated photoelectron spectra and data on the optical absorption indicates that the obtained films contain phases of stoichiometric SiO_2, nonstoichiometric silicon suboxides SiO_y, and amorphous silicon (Fig. 1). Silicon suboxides SiO_y consist of $SiSiO_3$, $SiSi_2O_2$, and $SiSi_3O$ tetrahedra, the presence of which is confirmed by the results of HRXPS measurements for $SiO_{1.4}$ films.

Figure 2 shows schematic two-dimensional (2D) energy diagrams of the (a) SiO_x structure and (b) potential fluctuations (according to the Shklovskii–Efros percolation theory) in heavily doped compensated semiconductor. The horizontal line A–A (Fig. 2a) indicates to what the energy diagram refers, the line E = 0 indicates the zero electron energy (vacuum energy level), E_g is the bandgap width of a-Si, E_c is the conduction-band bottom, and E_v is the valence-band top. Since E_g = 1.6 eV in a-Si, the minimum bandgap width in SiO_x also amounts to 1.6 eV. Increase in the bandgap width corresponds to growing content of sili-

Fig. 2. (a) Schematic 2D diagram of SiO_x structure and the energy diagram in *A–A* cross section; (b) potential fluctuations (according to the Shklovskii–Efros percolation theory) in heavily doped compensated semiconductor (μ is the Fermi level).

con suboxides. The maximum bandgap width in SiO_x is the same as that in SiO_2 (i.e., 8.0 eV). Taking into account that the electron affinity in a-Si is 3.6 eV and that in SiO_2 is 1 eV, and using the diagram in Fig. 2a, the maximum amplitude of potential fluctuations in SiO_x can be estimated as 2.6 eV for electrons and 3.8 eV for holes.

Figure 3 shows the experimental current–voltage characteristics (points) of $SiO_{1.4}$ and $SiO_{1.6}$ films in comparison to the results of calculations (solid lines) based on the Shklovskii–Efros percolation model [8]. This model has been previously used for the description of charge transport in nonstoichiometric HfO_x films [9]. In the present work, it is assumed that the random potential modulating the bandgap width has rather large amplitude. In this case, the quantum effects can be ignored and the boundary of delocalized states coincides with the percolation level [8]. The electric conductance in this system is determined by electrons thermoactivated to the delocalized states (for the sake of simplicity, the transport of holes is not considered). Then, according to theory [8], the current–voltage characteristics of disordered materials are described by the following expression:

$$J = J_0 \exp\left(-\frac{W_p^e - (CeaV_0^{(1-\gamma)/\gamma}F)^y}{kT}\right), \tag{3}$$

where J_0 is the preexponential factor, W_p^e is the percolation energy for electrons, $C = 0.25$ is a constant coefficient, $\gamma = 0.52$ is the critical index, a is the spatial scale of potential fluctuations, and V_0 is the amplitude of potential fluctuations. According to the Shklovskii–Efros percolation theory, the current–voltage characteristics of SiO_x are rectified in the J versus F^γ coordinates.

Fig. 3. Experimental current–voltage characteristics of SiO_x (points) measured at various temperatures and plotted in log$J$ vs. F^γ coordinates ($\gamma = 0.52$) in comparison to the results of model calculations (solid lines) for different SiO_x compositions: (a) $x = 1.4$; (b) $x = 1.6$.

The best coincidence of experiment and theory was obtained for the following sets of parameters. For $x = 1.4$ (Fig. 3a): $W_p^e = 0.5$ eV, $aV_0^{0.9} = 6.69 \times 10^{-7}$ cm eV$^{0.9}$, and $J_0 = 8$ A/cm^2; for $x = 1.6$ (Fig. 3b): $W_p^e = 0.8$ eV, $aV_0^{0.9} = 7.92 \times 10^{-7}$ cm eV$^{0.9}$, and $J_0 = 28$ A/cm^2. Then, using amplitude of potential fluctuations $V_0 = 2.6$ eV for electrons (Fig. 2a), we obtain the following estimations of the fluctuation scale: $a = 3.1$ nm for $x = 1.4$ and $a = 3.7$ nm for $x = 1.6$. Estimation of the specific conductivity by formula $\sigma_0 = J_0/F$ yields $\sigma_0 \approx 10^{-6}$ $(\Omega\ \text{cm})^{-1}$.

According to the Shklovskii–Efros model of potential fluctuations in compensated semiconductors [8], these fluctuations have an electrostatic nature and arise due to spatial inhomogeneity of the density of ionized (charged) donors and acceptors. In the original Shklovskii–Efros model, the bandgap width in a compensated semiconductor remains constant (Fig. 2b). According to the modified model proposed in the present work, the spatial fluctuations of potential are related to fluctuations of the chemical composition of SiO_x (Fig. 2a). Upon the generation of electron–hole pairs in a compensated semiconductor, the local electric field favors spatial separation of electron and hole (Fig. 2b). In SiO_x, the local electric field favors spatial proximity of an electron and hole, with their possible subsequent recombination (Fig. 2a). Thus, SiO_x can play the role of an effective radiative medium.

Acknowledgments. This study was supported in part by the Russian Science Foundation (project no. 18-49-08001) and the Ministry of Science and Technology (Taiwan, R.O.C.) grant MOST no. 107-2923-E-009-001-MY3.

REFERENCES

1. J. Kistner and M. B. Schubert, J. Appl. Phys. **114**, 193505 (2013).
2. S. Hernandez, P. Miska, M. Grun, S. Estrade, F. Peiro, B. Garrido, M. Vergnat, and P. Pellegrino, J. Appl. Phys. **114**, 233101 (2013).
3. F. Feldmann, M. Nicolai, R. Muller, C. Reichel, and M. Hermle, Energy Proc. **124**, 31 (2017).
4. N. V. Duy, S. Jung, K. Kim, D. N. Son, N. T. Nga, J. Cho, B. Choi, and J. Yi, J. Phys. D: Appl. Phys. **43**, 075101 (2010).
5. A. Mehonic, A. Vrajitoarea, S. Cueff, S. Hudziak, H. Howe, C. Labbe, R. Rizk, M. Pepper, and A. J. Kenyon, Sci. Rep. **3**, 1 (2013).
6. V. A. Gritsenko, Phys. Usp. **51**, 699 (2008).
7. J. P. Powell and M. Morad, J. Appl. Phys. **49**, 2499 (1978).
8. B. I. Shklovskii, Sov. Phys. Semicond. **13**, 53 (1979).
9. D. R. Islamov, V. A. Gritsenko, C. H. Cheng, and A. Chin, Appl. Phys. Lett. **105**, 262903 (2014).

Translated by P. Pozdeev